J. Opt. A: Pure Appl. Opt. **9** (2007) 593–602 doi:10.1088/1464-4258/9/7/009

Vector-mode analysis of symmetric two-point sources

Massimo Santarsiero[1,2], Franco Gori[1,2], Riccardo Borghi[2,3] and Giorgio Guattari[2,3]

[1] Dipartimento di Fisica, Università Roma Tre, Via della Vasca Navale 84, I-00146 Rome, Italy
[2] CNISM, Via della Vasca Navale 84, I-00146 Rome, Italy
[3] Dipartimento di Elettronica Applicata, Università Roma Tre, Via della Vasca Navale 84, I-00146 Rome, Italy

E-mail: santarsiero@fis.uniroma3.it

Received 20 March 2007, accepted for publication 25 April 2007
Published 19 June 2007
Online at stacks.iop.org/JOptA/9/593

Abstract
Vector modes and eigenvalues are evaluated for a partially coherent source when only a pair of points is of interest, as in the case of the radiation emerging from the pinholes of a Young interferometer fed by an electromagnetic beam. Analytical results are presented, paying particular attention to those cases when the fields at the two points cannot be distinguished from one another on the basis of their second-order correlation properties. It is shown that the superposition scheme provided by the vectorial modal theory of coherence allows a simple interpretation of the interference pattern and an intuitive understanding of its coherence–polarization features to be given. Examples are given for the case of electromagnetic Gaussian Schell-model sources.

Keywords: partially coherent electromagnetic sources, modal theory of coherence, Young interferometer

1. Introduction

In the scalar domain, Wolf's modal theory of coherence [1] has proved to represent a fundamental tool in studying and understanding the properties of partially coherent light sources. According to it, any partially coherent light source can be thought of as the incoherent superposition of a discrete number of perfectly coherent sources (the *modes*), each of them characterized by a specific value of the power it radiates. The analytical form of the modes and the values of the corresponding powers are obtained by finding eigenfunction and eigenvalues, respectively, of an integral operator whose kernel is the cross-spectral density (CSD) of the source. Thinking of the source as arising from the superposition of perfectly coherent sources has unquestionable advantages, for instance, whenever the propagation features of the radiated beam have to be investigated, or when a specific light source has to be synthesized [2]. On the other hand, analytical closed forms for the modes are found only in very particular, although significant, cases [3–9] and often approximate numerical techniques are to be adopted.

In recent years, a great deal of research has been devoted to the study of the so-called electromagnetic (or vector) partially coherent sources, for which the vectorial character of the electromagnetic field cannot be ignored. This is the case, for instance, of sources that are both partially coherent and partially polarized, or that present non-uniform polarization across the source plane. In such cases, in principle, the correlation functions among all the components of the electromagnetic field have to be considered [10] but, within the validity of the paraxial approximation, only the correlations between the two transverse components of the field (e.g. the electric one) are sufficient.

James [11] was the first who used a correlation tensor within the paraxial approximation for successfully predicting changes of the polarization degree on free-space propagation induced by partial correlation between the x and y components of the electric field. A few years later, a 2×2 matrix was introduced [12, 13], namely, the beam coherence–polarization (BCP for short) matrix, as the basic tool for the study of electromagnetic sources in the paraxial domain. In particular, in [13] it was also shown that generalized interference laws

can be established for the elements of the correlation matrix at the output plane of a Young interferometer, giving rise to an oscillatory behaviour of such elements. The original analysis about the BCP matrix was carried out in the space–time domain, and later it was also extended to the space–frequency domain by Wolf [14].

A further step in advancing toward a more complete theory was established, not long ago, through an extension in the temporal domain of Wolf's modal theory of coherence to the case of electromagnetic sources [15]. In analogy to the scalar case, the 2×2 correlation tensor plays the role of the kernel of a non-negative definite Hilbert–Schmidt integral operator, which now acts on a pair of functions, i.e. the x and y components of the electric field. Then, on invoking the spectral theorem, the modal decomposition follows. Modes and eigenvalues keep the same meaning as for the scalar case, but now a system of coupled integral equations must be solved in order for them to be found. In particular, the modes represent perfectly correlated vector field distributions, characterized by their own two-component Jones vectors [15]. Shortly after its introduction in the temporal domain, vectorial modal theory was also formulated in the spectral domain [16].

It should be stressed that the analytical problem of finding eigenvalues and eigenvectors of an assigned correlation tensor is much more difficult than for the scalar case, except of course when the polarization is uniform across the source [16], and closed-form expressions for modes and eigenvalues have been found only for a very few cases [15]. Nonetheless, if a pair of source points at a time is of interest, finding the modal expansion becomes quite elementary. The most important example of this situation occurs in the analysis of Young's interferometer. In fact, in the ideal case of very small pinholes [10], we can say that only two points of the field are selected. For want of a better name, we shall refer to such a situation as the case of *two-point sources*.

Due to the current interest for the Young interference experiment beyond the scalar approximation [17–24], it appears that finding the modal decomposition of the radiation emerging from the pinholes represents in itself a task of considerable conceptual importance. Moreover, the knowledge of the modal expansion can be of help in understanding the structure of the interference pattern and in elucidating the relationship between the coherence–polarization properties of the light at the pinholes as well as those in the fringe plane.

In [24] it was shown that the problem of the vector mode determination of a two-point source reduces to solving a secular problem for a 4×4 matrix, whose elements represent the correlations between the components of the field at the two points. The aim of the present paper is to apply the general results obtained in [24] to a class of two-point sources, i.e. those sources for which the two considered points are completely indistinguishable from one another on the basis of second-order correlation measurements performed on any pair of field components. This means, in particular, that all the coherence–polarization properties of the source remain the same if the fields at the two points are interchanged. We shall refer to such sources as *symmetric* two-point sources. This concept deserves some clarification.

Suppose we consider the electromagnetic field at two fixed points in space and we have to distinguish one point from the other. Of course, first we may detect some local quantities pertinent to the two fields, such as total intensity, polarization degree, polarization state of the polarized component, and so on. In other terms, we may measure the elements of the polarization matrices [2] of the field at the two points. But, even if the two matrices turn out to be identical, we can figure out some further way for distinguishing the two points. In fact, we may measure the correlations existing between each of the transverse components of the field at one point and those of the other one. It may happen, for instance, that the x component of the field at point 1 is perfectly correlated with the y component of the field at point 2, while the y component of the field at point 1 and the x component of the field at point 2 are mutually completely uncorrelated. So, measuring the correlation functions between orthogonal field components of the field at the two points provides a way to discriminate one point from the other. In contrast, the two points are completely indistinguishable (in the sense of the second-order coherence theory) if all the correlation functions between any pairs of field components take the same value after interchanging the two points.

It will be shown that simple analytical expressions are obtained for eigenvalues and modes of a symmetric two-point source and that several features of the electromagnetic field at the output plane of the interferometer (such as its intensity distribution, degree of polarization and behaviour of the Stokes parameters) can be easily interpreted in terms of superpositions of mutually uncorrelated perfectly polarized light beams. Nonetheless, as we shall see, significant two-point electromagnetic sources belong to this class.

As an important example of a symmetric two-point source we will consider a source obtained by letting an electromagnetic Gaussian Schell-model (EGSM) beam to feed a Young interferometer. EGSM beams, sometimes referred to as partially polarized Gaussian Schell-model (PGSM) beams, have been introduced as the natural extension of the scalar Gaussian Schell-model beams [2] to the vector case [11, 25, 26]. Since their introduction, EGSM beams have proved to represent a powerful tool for modelling partially coherent electromagnetic beams and studying their propagation [27–32]. They have also been employed to investigate the coherence and polarization properties of Young's interference pattern formed by stochastic electromagnetic beams [17, 20, 19, 23].

The paper is organized as follows. In section 2 the definition of the BCP matrix is recalled, together with its vector mode decomposition and the application to a two-point source. The case of a symmetric two-point source is studied in section 3 while examples are worked out in section 4.

2. Preliminaries

2.1. The BCP matrix and its vector mode decomposition

Within the framework of the paraxial approximation, one can account for the complete set of space–time correlation functions at two typical points $\mathbf{r}_1$ and $\mathbf{r}_2$ by using the BCP matrix [13], which is defined as the correlation matrix of the Jones vectors of the field at the points $\mathbf{r}_1$ and $\mathbf{r}_2$. More

precisely, if one introduces the Jones vector of the electric field at the coordinate $\mathbf{r}$ as the column vector

$$\mathbf{E}(\mathbf{r}, t) = \begin{bmatrix} E_x(\mathbf{r}, t) \\ E_y(\mathbf{r}, t) \end{bmatrix}, \tag{1}$$

the corresponding BCP matrix is defined as

$$\begin{aligned} \hat{J}(\mathbf{r}_1, \mathbf{r}_2) &= \langle \mathbf{E}(\mathbf{r}_1, t)\mathbf{E}^{\dagger}(\mathbf{r}_2, t)\rangle \\ &= \begin{bmatrix} J_{xx}(\mathbf{r}_1, \mathbf{r}_2) & J_{xy}(\mathbf{r}_1, \mathbf{r}_2) \\ J_{yx}(\mathbf{r}_1, \mathbf{r}_2) & J_{yy}(\mathbf{r}_1, \mathbf{r}_2) \end{bmatrix}, \end{aligned} \tag{2}$$

where the dagger denotes Hermitian conjugation and the angle brackets time average. Therefore, the elements of the BCP matrix give the cross-correlation between the α and β components ($\alpha, \beta = x, y$) of the electric field at points $\mathbf{r}_1$ and $\mathbf{r}_2$ for zero time delay. In the case of polychromatic fields, use should be made of the CSD tensor defined in the spectral domain [14], but the two definitions are equivalent if quasi-monochromatic sources are considered. Accordingly, we shall continue using the definition in equation (2), but our results could be easily transposed into the space–frequency domain.

The local properties of the beam are specified by the BCP matrix with $\mathbf{r}_1 = \mathbf{r}_2$, which coincides with the polarization (or coherence) matrix defined in [10]. In fact, the whole set of the Stokes parameters of the radiation can be evaluated starting from the values of the polarization matrix as follows [10]:

$$\begin{aligned} S_0 &= J_{xx} + J_{yy}; & S_1 &= J_{xx} - J_{yy}; \\ S_2 &= J_{xy} + J_{yx}; & S_3 &= i(J_{xy} - J_{yx}), \end{aligned} \tag{3}$$

where the matrix elements are evaluated with $\mathbf{r}_1 = \mathbf{r}_2$. In particular, the optical intensity and the degree of polarization at the coordinate $\mathbf{r}$ turn out to be

$$I(\mathbf{r}) = \mathrm{Tr}\{\hat{J}(\mathbf{r}, \mathbf{r})\} = S_0(\mathbf{r}) \tag{4}$$

and

$$P(\mathbf{r}) = \sqrt{1 - \frac{4\,\mathrm{Det}\{\hat{J}(\mathbf{r}, \mathbf{r})\}}{[\mathrm{Tr}\{\hat{J}(\mathbf{r}, \mathbf{r})\}]^2}} = S_0^{-1}(\mathbf{r}) \sqrt{\sum_{n=0}^{3} S_n^2(\mathbf{r})}, \tag{5}$$

respectively, where Det stands for determinant and Tr for trace.

Following the same path that leads to the definition of the coherent modes of a scalar cross-spectral density [1], it is possible to define the vector modes of a BCP matrix. In particular, it has been shown [15, 16] that, under very general hypotheses, for any partially coherent vector source the elements of the BCP matrix can be expanded into a series of modes, to be found by solving the following pair of coupled integral equations:

$$\begin{gathered} \sum_{\beta} \int J_{\alpha,\beta}(\mathbf{r}, \mathbf{r}')\varphi_{n,\beta}(\mathbf{r}')\mathrm{d}^2 r' = \Lambda_n \varphi_{n,\alpha}(\mathbf{r}); \\ (\alpha = x, y; n \text{ integer}), \end{gathered} \tag{6}$$

where the integration is performed across the whole transverse plane.

A more compact form for equation (6) can be given if one arranges the two components of a mode into a column vector, i.e.

$$\mathbf{\Phi}_n(\mathbf{r}) = \begin{bmatrix} \varphi_{n,x}(\mathbf{r}) \\ \varphi_{n,y}(\mathbf{r}) \end{bmatrix}, \tag{7}$$

so that the above pair of coupled integral equations takes the form

$$\int \hat{J}(\mathbf{r}, \mathbf{r}')\mathbf{\Phi}_n(\mathbf{r}')\,\mathrm{d}^2 r' = \Lambda_n \mathbf{\Phi}_n(\mathbf{r}), \tag{8}$$

which is perfectly analogous to its scalar version [2]. Λ_n and $\mathbf{\Phi}_n(\mathbf{r})$ are the eigenvalues and the eigenfunctions, respectively, of the BCP matrix and, due to the non-negative character of $\hat{J}(\mathbf{r}, \mathbf{r}')$, it turns out that $\Lambda_n \geqslant 0$ for any n. Furthermore, from the definition of vector modes, a Mercer expansion can be used to represent the BCP matrix, namely,

$$\hat{J}(\mathbf{r}_1, \mathbf{r}_2) = \sum_n \Lambda_n \mathbf{\Phi}_n(\mathbf{r}_1)\mathbf{\Phi}_n^{\dagger}(\mathbf{r}_2). \tag{9}$$

The latter equation can be read as follows. Any partially polarized, partially coherent source can be thought of as obtained from the incoherent superposition of a discrete (possibly infinite) number of perfectly correlated and perfectly polarized fields, represented by their Jones vectors $\mathbf{\Phi}_n(\mathbf{r})$. The power carried by each mode is proportional to the corresponding eigenvalue.

2.2. *Vector mode decomposition of a two-point source*

We are interested here in the case in which the modal theory of coherence is applied to a pair of fixed points, as for the radiation emerging from the two pinholes of a Young interferometer, if the latter are approximated by two pointlike apertures [24]. Under this approximation, a typical time fluctuating field component, say $E_\alpha(\mathbf{r}, t)$ ($\alpha = x, y$) emerging from the mask can be written as a pair of Dirac δ functions centred at the pinholes' locations, say $\mathbf{p}_i$ ($i = 1, 2$), so that

$$E_\alpha(\mathbf{r}, t) = S \sum_{i=1,2} E_\alpha^i(t)\delta(\mathbf{r} - \mathbf{p}_i), \tag{10}$$

where $E_\alpha^i(t) = E_\alpha(\mathbf{p}_i, t)$ denotes the value of the α component of the field sampled by the ith pinhole, whereas S is a proportionality factor that has the dimensions of an area. As is well known, factors of this type are to be introduced whenever Dirac functions are used. Similarly, the elements of the BCP matrix can be expressed as

$$J_{\alpha\beta}(\mathbf{r}_1, \mathbf{r}_2) = S^2 \sum_{i,j=1,2} J_{\alpha\beta}^{ij}\delta(\mathbf{r}_1 - \mathbf{p}_i)\delta(\mathbf{r}_2 - \mathbf{p}_j), \tag{11}$$

where $J_{\alpha\beta}^{ij} = J_{\alpha\beta}(\mathbf{p}_i, \mathbf{p}_j)$ denotes the (generally complex) element of the BCP matrix relating to the α and β components of the field at the points $\mathbf{p}_i$ and $\mathbf{p}_j$ ($\alpha, \beta = x, y$; $i, j = 1, 2$).

Let us write the Cartesian components of the modes in a form similar to that in equation (10), namely

$$\varphi_{n,\alpha}(\mathbf{r}) = S \sum_{i=1,2} \varphi_{n,\alpha}^i \delta(\mathbf{r} - \mathbf{p}_i), \tag{12}$$

and insert it into equation (6) together with equation (11). We then find

$$S \sum_{\beta=x,y} \sum_{i,j=1,2} J_{\alpha\beta}^{ij}\varphi_{n,\beta}^j \delta(\mathbf{r} - \mathbf{p}_i) = \Lambda_n \sum_{i=1,2} \varphi_{n,\alpha}^i \delta(\mathbf{r} - \mathbf{p}_i), \tag{13}$$

for $\alpha = x, y$. This, in turn, requires the following equations to be satisfied:

$$\sum_{\beta=x,y} \sum_{j=1,2} J_{\alpha\beta}^{ij}\varphi_{n,\beta}^j = \lambda_n \varphi_{n,\alpha}^i, \tag{14}$$

where $\lambda_n = \Lambda_n/S$. Equation (14) represents a 4×4 system of linear homogeneous equations.

To simplify the formalism, it is convenient to introduce four-component column vectors to be representative of the electric field vectors at the two points. In particular, we have

$$\mathcal{E}(t) = \begin{bmatrix} \mathbf{E}_1(t) \\ \mathbf{E}_2(t) \end{bmatrix} = \begin{bmatrix} E_x^{(1)}(t) \\ E_y^{(1)}(t) \\ E_x^{(2)}(t) \\ E_y^{(2)}(t) \end{bmatrix}, \tag{15}$$

where $\mathbf{E}_i(t)$ $(i = 1, 2)$ denotes the Jones vector of the transverse electromagnetic field at the point located at $\mathbf{p}_i$ and $E_\alpha^{(i)}(t)$ $(\alpha = x, y)$ are its Cartesian components. Accordingly, a 4×4 correlation matrix, say $\hat{\rho}$, can be defined as

$$\hat{\rho} = \langle \mathcal{E}(t)\mathcal{E}^\dagger(t) \rangle = \begin{bmatrix} \hat{J}_{11} & \hat{J}_{12} \\ \hat{J}_{12}^\dagger & \hat{J}_{22} \end{bmatrix}, \tag{16}$$

where $\hat{J}_{ij} = \langle \mathbf{E}_i(t)\mathbf{E}_j^\dagger(t) \rangle$ $(i, j = 1, 2)$ is the BCP matrix evaluated at the points i and j.[4]

In an analogous way, the modes of the source will be expressed as four-component vectors. With evident meaning of the symbols we then have

$$\mathbf{\Psi}_n = \begin{bmatrix} \mathbf{\Phi}_{n,1} \\ \mathbf{\Phi}_{n,2} \end{bmatrix} = \begin{bmatrix} \varphi_{n,x}^{(1)} \\ \varphi_{n,y}^{(1)} \\ \varphi_{n,x}^{(2)} \\ \varphi_{n,y}^{(2)} \end{bmatrix}, \tag{17}$$

so that the homogeneous linear system in equation (14) can be written in matrix form as

$$\hat{\rho}\mathbf{\Psi}_n = \lambda_n \mathbf{\Psi}_n, \tag{18}$$

and it is clear that finding the modal expansion of the source corresponds to evaluating eigenvalues and eigenvectors of the complex-valued matrix $\hat{\rho}$. Since the BCP matrix is non-negative definite [13], there will be four non-negative eigenvalues and four mutually orthogonal eigenvectors (each of them with four elements), for which we can write

$$\mathbf{\Psi}_n^\dagger \mathbf{\Psi}_m = \mathbf{\Phi}_{n,1}^\dagger \mathbf{\Phi}_{m,1} + \mathbf{\Phi}_{n,2}^\dagger \mathbf{\Phi}_{m,2} = \delta_{n,m}, \tag{19}$$

with $\delta_{n,m}$ being the Kronecker symbol. Mercer's expansion of the matrix $\hat{\rho}$ is then

$$\hat{\rho} = \sum_n \lambda_n \mathbf{\Psi}_n \mathbf{\Psi}_n^\dagger. \tag{20}$$

From a physical point of view, each of the modes represents a perfectly correlated field distribution at the pinholes, and any field distribution at the pinholes can be obtained by superimposing four such modes in an uncorrelated way. More precisely, one needs at most four modes because, in certain cases, one or more eigenvalues may vanish.

On the other hand, all the characteristics of the radiation across the observation plane of the Young interferometer, i.e. across its output plane, can be deduced from a superposition scheme involving the vector modes of the BCP matrix at the pinholes. In particular, since the modes are mutually uncorrelated, the polarization matrix at any point of the observation plane can be written as the sum of the polarization matrices produced at that point by each of the modes. The corresponding Stokes parameters, as well as the polarization degree at any point of the interference pattern, can be deduced from its elements using equations (3)–(5).

For a typical 4×4 Hermitian matrix, eigenvalues and eigenvectors can be numerically evaluated even with a hand-held computer. Accordingly, the modal expansion for a two-point source is particularly easy. In principle, eigenvalues can always be evaluated in closed form, by solving the fourth-order secular equation through Cardano's formula. While in general the resulting expressions are rather cumbersome, we shall see later on that, in a number of cases, the analytical formulae are simple enough.

Let us come back briefly to the form of the correlation matrix in equation (16). Its diagonal blocks, $\hat{J}_{ii}$, coincide with the polarization matrices at the two points of the Young interferometer and must necessarily be Hermitian and non-negative definite [10]. Intensity and degree of polarization at every point can be evaluated from equations (4) and (5). In particular, the sum of the intensities of the field at the pinholes can be evaluated (apart from the proportionality factor S) as the trace of the matrix $\hat{\rho}$, which, in turn, equals the sum of the four eigenvalues:

$$I_{\text{tot}} = \text{Tr}\{\hat{\rho}\} = \sum_n \lambda_n. \tag{21}$$

On the other hand, the off-diagonal blocks, accounting for the correlations between the field components at point 1 and point 2, need not be Hermitian.

The Mercer expansion in equation (20) allows analogous expansions for the four blocks of the matrix $\hat{\rho}$ to be written. In fact, on substituting from equation (17) into equation (20) we obtain at once the following expression for each of the blocks:

$$\hat{J}_{ij} = \sum_n \lambda_n \mathbf{\Phi}_{n,i} \mathbf{\Phi}_{n,j}^\dagger. \tag{22}$$

This, in particular, means that the diagonal elements $\hat{J}_{ii}$ $(i = 1, 2)$ are given by

$$\hat{J}_{ii} = \sum_n \lambda_n \mathbf{\Phi}_{n,i} \mathbf{\Phi}_{n,i}^\dagger, \tag{23}$$

which resembles a scalar Mercer's expansion. One could be tempted to identify $\mathbf{\Phi}_{n,i}$ with the eigenvectors of the diagonal blocks. This, of course, cannot be done because the two-element vectors $\mathbf{\Phi}_{n,i}$ are not, in general, mutually orthogonal. However, from equation (23) we see at once that the traces of $\hat{J}_{ii}$ are given by

$$I_i = \text{Tr}\{\hat{J}_{ii}\} = \sum_n \lambda_n \mathbf{\Phi}_{n,i}^\dagger \mathbf{\Phi}_{n,i}, \tag{24}$$

where $\mathbf{\Phi}_{n,i}^\dagger \mathbf{\Phi}_{n,i}$ is nothing but the norm of the subvectors $\mathbf{\Phi}_{n,i}$.

As far as the antidiagonal block is concerned, from equation (22) we have

$$\hat{J}_{12} = \sum_n \lambda_n \mathbf{\Phi}_{n,1} \mathbf{\Phi}_{n,2}^\dagger, \tag{25}$$

and

$$\text{Tr}\{\hat{J}_{12}\} = \sum_n \lambda_n \mathbf{\Phi}_{n,2}^\dagger \mathbf{\Phi}_{n,1}, \tag{26}$$

where $\mathbf{\Phi}_{n,2}^\dagger \mathbf{\Phi}_{n,1}$ is the inner product between the two halves of $\mathbf{\Psi}_n$. It should be noted that a similar decomposition has recently been proposed by Kim and Wolf [33].

[4] The 4×4 correlation matrix defined in [24], therein denoted by $\hat{T}$, is obtained from $\hat{\rho}$ after a suitable permutation of its elements.

3. Application to symmetric two-point sources

3.1. Symmetric two-point sources

A particular, although rather important, class of two-point sources is the one comprising those sources for which the two points are completely equivalent, as far as their coherence–polarization properties are concerned. This means, for instance, that the polarization matrices of the fields at the holes are identical, but also that one cannot distinguish one field from the other on the basis of correlation measurement involving both the holes. In other words, all the correlation functions pertinent to the components of the electric field, namely, $J^{ij}_{\alpha\beta}$ $(i, j = 1, 2; \alpha, \beta = x, y)$ are required to remain unchanged on interchanging the indices i and j. This may appear a rather severe requirement, but we shall see that significant examples of sources belong to such a class. On the other hand, very simple expressions are obtained for eigenvalues and modes of symmetric two-point sources.

From a mathematical point of view, a symmetric two-point source is characterized from the fact that $J^{ij}_{\alpha\beta} = J^{ji}_{\alpha\beta} = (J^{ij}_{\beta\alpha})^*$, where the asterisk denotes complex conjugation and the latter equality being a consequence of the definition of $J^{ij}_{\alpha\beta}$ [13]. This means that all the four submatrices $\hat{J}_{ij}$ appearing in equation (16) are Hermitian. In particular, the diagonal elements of every submatrix are real while the off-diagonal ones are mutually complex conjugated. Then, the corresponding $\hat{\rho}$ matrix takes the form

$$\hat{\rho} = \begin{bmatrix} a & c & \alpha & \gamma \\ c^* & b & \gamma^* & \beta \\ \alpha & \gamma & a & c \\ \gamma^* & \beta & c^* & b \end{bmatrix}. \tag{27}$$

The parameters appearing in equation (27) cannot be chosen at will, because they must guarantee that certain requirements are met. First of all, since the diagonal blocks, $\hat{J}_{ii} (i = 1, 2)$, coincide with the polarization matrices at the two points of the Young interferometer, they must necessarily be Hermitian and non-negative definite [10]. In particular, this implies that a and b are real non-negative quantities while the Schwartz inequality fixes an upper bound for the modulus of the complex number c, namely

$$|c| \leqslant \sqrt{ab}. \tag{28}$$

For the class of sources considered here, even the off-diagonal blocks, $\hat{J}_{ij} (i \neq j)$, accounting for the correlations between the field components at the two points, are Hermitian, but they need not be positive semidefinite, so that α and β are real quantities but they may also be negative. The Schwartz inequality, applied to the elements of such blocks, gives

$$|\alpha| \leqslant a; \qquad |\beta| \leqslant b; \qquad |\gamma| \leqslant \sqrt{ab}. \tag{29}$$

Moreover, since the whole $\hat{\rho}$ matrix has to be non-negative definite [24], all its eigenvalues are required to be greater than or equal to zero. This imposes further constraints to the choices of the parameters appearing in equation (27), as we shall see in the following.

It is worthwhile to stress that, due to the form of the matrix in equation (27), the fields at the two pinholes are characterized by the same polarization matrix. In particular, they have the same intensity, i.e.

$$I_{\mathrm{ph}} = a + b, \tag{30}$$

and the same polarization degree, namely,

$$P_{\mathrm{ph}} = \frac{\sqrt{(a-b)^2 + 4|c|^2}}{(a+b)} \tag{31}$$

which, from equation (28), is seen to be bounded between 0 and 1.

3.2. Modal expansion of a symmetric two-point source

Here, the modal structure of a symmetric two-point source will be deduced, evaluating eigenvalues and modes of the $\hat{\rho}$ matrix in equation (27).

The eigenvalues of $\hat{\rho}$ can be calculated in closed form directly by solving the pertinent secular equation. In the case of the matrix in equation (27), some algebraic manipulations lead to the following result:

$$\begin{aligned} \lambda_1 &= \frac{Q_+ + R_+}{2}, & \lambda_2 &= \frac{Q_+ - R_+}{2}, \\ \lambda_3 &= \frac{Q_- + R_-}{2}, & \lambda_4 &= \frac{Q_- - R_-}{2}, \end{aligned} \tag{32}$$

where the quantities $Q_\pm$ and $R_\pm$ have been defined as

$$\begin{aligned} Q_\pm &= (a+b) \pm (\alpha+\beta); \\ R_\pm &= \sqrt{[(a-b) \pm (\alpha-\beta)]^2 + 4\,|c \pm \gamma|^2}, \end{aligned} \tag{33}$$

respectively.

The eigenvalues are required to be positive, so that it must be $Q_\pm \geqslant R_\pm$. This imposes further conditions on the values the parameters can assume. In particular, after simple algebra the non-negativity condition of the $\hat{\rho}$ matrix turns out to be the following:

$$\frac{|c \pm \gamma|^2}{(a \pm \alpha)(b \pm \beta)} \leqslant 1, \tag{34}$$

which, together with equations (28) and (29), will be taken for granted from now on.

Once the four eigenvalues are known, also the eigenvectors of the matrix $\hat{\rho}$ can be analytically evaluated by solving four linear systems. After some algebraic manipulation, they turn out to be

$$\begin{aligned} \boldsymbol{\Psi}_1 &= N_+ \begin{bmatrix} \phi_+ \\ 1 \\ \phi_+ \\ 1 \end{bmatrix}; & \boldsymbol{\Psi}_2 &= N_+ \begin{bmatrix} 1 \\ -\phi_+^* \\ 1 \\ -\phi_+^* \end{bmatrix}; \\ \boldsymbol{\Psi}_3 &= N_- \begin{bmatrix} \phi_- \\ 1 \\ -\phi_- \\ -1 \end{bmatrix}; & \boldsymbol{\Psi}_4 &= N_- \begin{bmatrix} 1 \\ -\phi_-^* \\ -1 \\ \phi_-^* \end{bmatrix}, \end{aligned} \tag{35}$$

where $\phi_\pm$ is given by

$$\phi_\pm = \frac{(a-b) \pm (\alpha-\beta) + R_\pm}{2(c \pm \gamma)^*}, \tag{36}$$

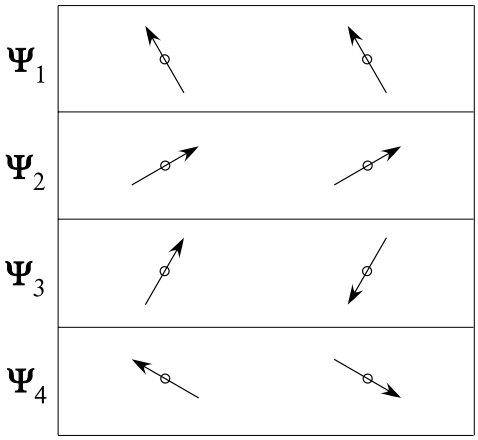

Figure 1. Polarization, supposed linear, of the modes at the two Young holes.

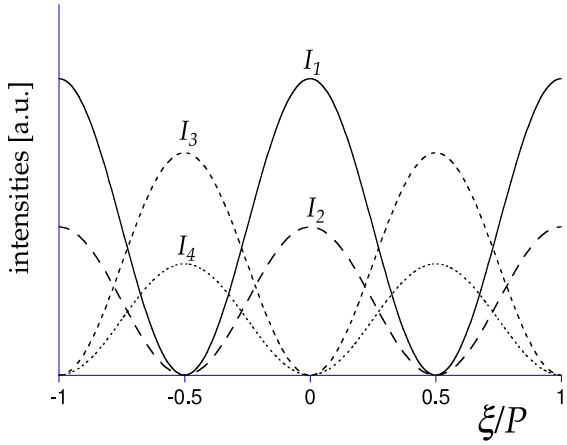

Figure 2. Intensities produced across the output plane by the four modes. P denotes the fringe period.

and

$$N_{\pm} = \frac{1}{\sqrt{2(1+|\phi_{\pm}|^2)}} \tag{37}$$

is a normalization factor.

On examining equation (35), we note several general characteristics of the modes. First of all, their power is evenly distributed between the two holes. Furthermore, the polarization state of all the modes is the same at the two points, i.e. the modes are uniformly polarized. Such considerations allow us to identify the polarization state of each of the modes by the Jones vector ($\mathbf{\Phi}_{n,1}$) pertinent to the field emerging from one of the Young pinholes.

Moreover, although the polarization state of the modes depends on the choice of the parameters, the first two modes are always mutually orthogonal (i.e. $\mathbf{\Phi}_{1,1}^{\dagger}\mathbf{\Phi}_{2,1} = 0$) and the same happens for the last two modes ($\mathbf{\Phi}_{3,1}^{\dagger}\mathbf{\Phi}_{4,1} = 0$), even though (in general) their polarization are different. Figure 1 shows the polarization (which is supposed to be linear, for convenience of representation) of typical mode fields in correspondence with the Young holes.

As a further consequence of the analytical form of the modes, the fields emerging from the two pinholes are in phase for the modes $\mathbf{\Psi}_1$ and $\mathbf{\Psi}_2$, while they are in opposition for the modes $\mathbf{\Psi}_3$ and $\mathbf{\Psi}_4$. Such relations are made evident in figure 1 by the arrow directions. Some general consequences of the above properties will be derived in section 3.3.

3.3. Coherence–polarization properties of the interference pattern

In the present case, due to the properties of the modes obtained in the previous subsection, some general features of the radiation across the observation plane can be deduced at once. First of all we note that, across the output plane of the interferometer, each of the modes gives rise to a sinusoidally varying field distribution. In particular, the Jones vector of the output field due to the modes $\mathbf{\Psi}_1$ and $\mathbf{\Psi}_2$ will be of the form $\mathbf{\Phi}_{i,1}\cos(K\xi)$; $(i = 1, 2)$, while, for the remaining two modes it will be $\mathbf{\Phi}_{i,1}\sin(K\xi)$; $(i = 3, 4)$, where ξ is the transverse coordinate across the output plane and K gives an account of the period of the fringe pattern. The intensities corresponding to the four modes, I_i $(i = 1, 2, 3, 4)$, could appear as in figure 2, where they are plotted for a typical case as functions of the reduced coordinate ξ/P, with $P = 2\pi/K$ being the fringe period.

More, in general, from the lack of correlation among the modes, the polarization matrix at the transverse coordinate ξ turns out to be

$$\hat{J}_{\text{out}}(\xi,\xi) = \left(\lambda_1\mathbf{\Phi}_{1,1}\mathbf{\Phi}_{1,1}^{\dagger} + \lambda_2\mathbf{\Phi}_{2,1}\mathbf{\Phi}_{2,1}^{\dagger}\right)\cos^2(K\xi) + \left(\lambda_3\mathbf{\Phi}_{3,1}\mathbf{\Phi}_{3,1}^{\dagger} + \lambda_4\mathbf{\Phi}_{4,1}\mathbf{\Phi}_{4,1}^{\dagger}\right)\sin^2(K\xi). \tag{38}$$

It is easily seen that each of the elements of $\hat{J}_{\text{out}}$ presents oscillations with respect to ξ, in agreement with the generalized interference laws derived in [13]. The same behaviour is exhibited, of course, by the Stokes parameters of the field [21, 22], which are linear combinations of the matrix elements.

In particular, the intensity distribution, corresponding to the Stokes parameter S_0, turns out to be

$$I_{\text{out}}(\xi) = \text{Tr}\{\hat{J}_{\text{out}}(\xi,\xi)\} = (\lambda_1+\lambda_2)\cos^2(K\xi) + (\lambda_3+\lambda_4)\sin^2(K\xi), \tag{39}$$

and it is seen to consist of two fringe patterns: one of them, with power given by $\lambda_1+\lambda_2$, is centred on the axis, while the other one, with power $\lambda_3+\lambda_4$, is laterally shifted by half a period (see figure 2).

At the centre of the interference pattern ($\xi = 0$) only the first two modes contribute to the total intensity, which turns out to be proportional to $\lambda_1+\lambda_2$. More precisely,

$$I_{\text{out}}(0) = \lambda_1+\lambda_2 = Q_+ = (a+b)+(\alpha+\beta). \tag{40}$$

Moreover, since $\lambda_1+\lambda_2 \geqslant \lambda_3+\lambda_4$ [as can be deduced from equation (32)], the central point of the fringe pattern is a maximum of the intensity distribution, while the minimum is reached half a period away from the maximum and equals $\lambda_3+\lambda_4$. This means that the visibility of the fringe pattern turns out to be

$$V_{\text{out}} = \frac{I_{\max}-I_{\min}}{I_{\max}+I_{\min}} = \frac{\lambda_1+\lambda_2-(\lambda_3+\lambda_4)}{\lambda_1+\lambda_2+(\lambda_3+\lambda_4)} = \frac{\alpha+\beta}{a+b}, \tag{41}$$

regardless of the values of c and γ.

Such a value of visibility coincides with the modulus of the degree of coherence that would be measured by means of the Young interferometer if the vectorial character of the radiation was neglected and no anisotropic optical elements were used in the detection process [13, 14]. It should be mentioned that other quantities have been defined to quantify the correlations among the field components of an electromagnetic field at two points, which are not always related to the visibility of the fringes in the interference pattern of a Young interferometer [34, 16, 18, 35, 36]. Some of these quantities, in particular, can be easily expressed in terms of the eigenvalues of the $\hat{\rho}$ matrix [16, 35].

As far as the three remaining Stokes parameters are concerned, since the values of their 'visibilities' depend on the specific polarization states of the modes, they will be discussed in the section devoted to the examples.

The knowledge of the vector modal structure of the field emerging from the pinholes allows one to evaluate also the degree of polarization of the radiation across the observation plane. Although the behaviour of such a quantity as a function of the transverse coordinate depends on the particular form of the modes and, in particular, on their polarization states, in the present case the value it takes at the central point of the fringe pattern can be evaluated at once, from the eigenvalues alone. In fact, since only the first two modes contribute to the on-axis intensity and such two modes have orthogonal polarizations, the axial degree of polarization turns out to be

$$P_{\mathrm{out}}(0) = \frac{\lambda_1 - \lambda_2}{\lambda_1 + \lambda_2} = \frac{R_+}{Q_+} = \frac{\sqrt{[(a-b)+(\alpha-\beta)]^2 + 4\,|c+\gamma|^2}}{(a+b)+(\alpha+\beta)}, \qquad (42)$$

which generally differs from that at the pinholes (equation (31)). The dependence of the axial degree of polarization on the coherence properties of the radiation impinging on the Young mask has been the subject of some recent work [17, 19]. Incidentally, we note that the requirement that the axial degree of polarization be a quantity less than unity is always fulfilled, due to the condition in equation (34).

In section 4, the above results will be applied to the case of a two-point EGSM source and it will be shown in detail how the knowledge of the modal structure of the field emerging from a Young interferometer can be used to get information about the coherence–polarization properties of the interference field.

4. Modal expansion of a two-point EGSM source

4.1. Two-point EGSM sources

We recall that the mutual intensity of an ordinary, scalar GSM source, say $J_{\mathrm{sc}}(\mathbf{r}_1, \mathbf{r}_2)$, takes the form [2]

$$J_{\mathrm{sc}}(\mathbf{r}_1, \mathbf{r}_2) = I_0 \exp\left[-\frac{\left(r_1^2 + r_2^2\right)}{4\sigma^2} - \frac{(\mathbf{r}_1 - \mathbf{r}_2)^2}{2\delta^2}\right], \qquad (43)$$

where I_0 is a constant intensity factor, while σ and δ are the widths of the intensity profile and the degree of coherence, respectively.

EGSM sources have been defined [26] as those sources for which all the elements of the pertaining BCP matrices are of the form of equation (43). More explicitly, we have (with $\alpha, \beta = x, y$)

$$J_{\alpha\beta}(\mathbf{r}_1, \mathbf{r}_2) = I_{\alpha\beta} \exp\left[-\frac{\left(r_1^2 + r_2^2\right)}{4\sigma_{\alpha\beta}^2} - \frac{(\mathbf{r}_1 - \mathbf{r}_2)^2}{2\delta_{\alpha\beta}^2}\right]. \qquad (44)$$

Hermiticity of $\hat{J}(\mathbf{r}, \mathbf{r}')$ requires [13, 26, 31] that I_{xx} and I_{yy} are real quantities, while $I_{xy} = I_{yx}^*$. However, the argument of I_{xy} gives account of a phase difference between the x and the y component of the field, which could be easily removed by means of a suitable retarder. Without loss of generality, it is then customary to take I_{xy} as real and positive as well, so that $I_{xy} = I_{yx} \geqslant 0$. It also follows from the Hermiticity of the BCP matrix that $\sigma_{xy} = \sigma_{yx}$ and $\delta_{xy} = \delta_{yx}$. Moreover, for simplicity we use the hypothesis that $\sigma_{\alpha\beta} = \sigma$; $(\alpha, \beta = x, y)$.

Further constraints come from the fact that $\hat{J}(\mathbf{r}, \mathbf{r}')$ has to be non-negative definite [13]. It has been found, for instance, that a sufficient condition ensuring positive semidefiniteness is the following [26, 31]:

$$\max\left\{\delta_{xx}, \delta_{yy}\right\} \leqslant \delta_{xy} \leqslant \min\left\{\delta_{xx}, \delta_{yy}\right\} \sqrt{\frac{\sqrt{I_{xx} I_{yy}}}{I_{xy}}}. \qquad (45)$$

In conclusion, the BCP matrix of the EGSM source has the form

$$\hat{J}(\mathbf{r}_1, \mathbf{r}_2) = \exp\left(-\frac{r_1^2 + r_2^2}{4\sigma^2}\right) \times \begin{bmatrix} I_{xx} \exp[-\frac{(\mathbf{r}_1 - \mathbf{r}_2)^2}{2\delta_{xx}^2}] & I_{xy} \exp[-\frac{(\mathbf{r}_1 - \mathbf{r}_2)^2}{2\delta_{xy}^2}] \\ I_{xy} \exp[-\frac{(\mathbf{r}_1 - \mathbf{r}_2)^2}{2\delta_{xy}^2}] & I_{yy} \exp[-\frac{(\mathbf{r}_1 - \mathbf{r}_2)^2}{2\delta_{yy}^2}] \end{bmatrix}. \qquad (46)$$

Now we can apply the vector-mode theory of coherence to the case in which a EGSM beam impinges onto the mask of a Young interferometer. For simplicity, we shall suppose the pinholes to be located at $\mathbf{p}_1 = (x, 0)$ and $\mathbf{p}_2 = (-x, 0)$. So, from equation (16), the corresponding $\hat{\rho}$ matrix has just the form of equation (27), apart from the overall factor $I_{yy} \exp(-x^2/2\sigma^2)$, with parameters given by

$$\begin{aligned} a &= I_{xx}/I_{yy}; \qquad b = 1; \\ c &= c^* = I_{xy}/I_{yy}; \qquad \alpha = (I_{xx}/I_{yy})\mu_{xx}; \\ \beta &= \mu_{yy}; \qquad \gamma = \gamma^* = (I_{xy}/I_{yy})\mu_{xy}, \end{aligned} \qquad (47)$$

where, for brevity, the following quantities have been introduced:

$$\mu_{xx} = \exp\left(-\frac{2x^2}{\delta_{xx}^2}\right); \qquad \mu_{yy} = \exp\left(-\frac{2x^2}{\delta_{yy}^2}\right); \qquad \mu_{xy} = \exp\left(-\frac{2x^2}{\delta_{xy}^2}\right), \qquad (48)$$

which represent the normalized correlation functions among the transversal components of the field at the two points.

Of course, all considerations made in section 3 are applicable to such a choice of the parameters. In particular, the intensity of the fields emerging from each of the pinholes turns out to be

$$I_{\mathrm{ph}} = 1 + a, \qquad (49)$$

and the polarization degree at the pinholes is

$$P_{\rm ph} = \frac{\sqrt{(a-1)^2 + 4c^2}}{(a+1)}. \tag{50}$$

Moreover, all the components of the modes (equations (35) and (36)) take real values, so that the modes are linearly polarized. A more detailed analysis of the modal structure of the two-point EGSM source and of its consequences to the coherence–polarization properties of the fringe pattern will be presented in sections 4.2 and 4.3, where some particular choices of the parameters will be discussed.

4.2. Orthogonal field components with equal power

Here we consider the case $a = b = 1$ and $\mu_{xx} = \mu_{yy}$. This corresponds to taking radiation having components along x and y with the same power at the Young holes, and with $\delta_{xx} = \delta_{yy}$. Therefore, this case reduces to that considered in [17], where the relationship between degree of coherence and degree of polarization at the central point of a Young interference pattern was first studied, and that of [20], where the coherence–polarization features of the radiation were investigated across the whole pattern.

We can evaluate eigenvalues and modes from the general expressions given in section 3.2, thus obtaining

$$Q_\pm = 2(1 \pm \mu_{xx});\ R_\pm = 2c(1 \pm \mu_{xy}), \tag{51}$$

so that the eigenvalues turn out to be

$$\begin{aligned} \lambda_1 &= 1 + \mu_{xx} + c(1 + \mu_{xy}), \\ \lambda_2 &= 1 + \mu_{xx} - c(1 + \mu_{xy}), \\ \lambda_3 &= 1 - \mu_{xx} + c(1 - \mu_{xy}), \\ \lambda_4 &= 1 - \mu_{xx} - c(1 - \mu_{xy}). \end{aligned} \tag{52}$$

Furthermore, from equation (36) we have $\phi_\pm = 1$, so that the modes are given by

$$\begin{aligned} \mathbf{\Psi}_1 &= \frac{1}{2}\begin{bmatrix} 1 \\ 1 \\ 1 \\ 1 \end{bmatrix}, \qquad \mathbf{\Psi}_2 = \frac{1}{2}\begin{bmatrix} 1 \\ -1 \\ 1 \\ -1 \end{bmatrix}, \\ \mathbf{\Psi}_3 &= \frac{1}{2}\begin{bmatrix} 1 \\ 1 \\ -1 \\ -1 \end{bmatrix}, \qquad \mathbf{\Psi}_4 = \frac{1}{2}\begin{bmatrix} 1 \\ -1 \\ -1 \\ 1 \end{bmatrix}. \end{aligned} \tag{53}$$

The modes $\mathbf{\Psi}_1$ and $\mathbf{\Psi}_3$ are polarized along a line at $\pi/4$ in the xy plane, while $\mathbf{\Psi}_2$ and $\mathbf{\Psi}_4$ are polarized at $-\pi/4$.

Using equations (38), (52), and (3) the polarization matrix across the observation plane turns out to be

$$\hat{J}_{\rm out}(\xi, \xi) = \begin{bmatrix} 1 + \mu_{xx}\cos(2K\xi) & c[1 + \mu_{xy}\cos(2K\xi)] \\ c[1 + \mu_{xy}\cos(2K\xi)] & 1 + \mu_{xx}\cos(2K\xi) \end{bmatrix}, \tag{54}$$

that allows one to completely characterize the radiation in a point of the fringe pattern. In particular, from equation (3), the Stokes parameters can be evaluated as functions of the transverse coordinate as

$$\begin{aligned} S_0(\xi) &= 2\,[1 + \mu_{xx}\cos(2K\xi)]; \qquad S_1(\xi) = 0; \\ S_2(\xi) &= 2c\left[1 + \mu_{xy}\cos(2K\xi)\right]; \qquad S_3(\xi) = 0, \end{aligned} \tag{55}$$

and are shown to present typical sinusoidal oscillations around an average value [21], which are reminiscent of the analogous behaviour of the elements of the polarization matrix [13].

As far as the degree of polarization is concerned, in the present case we obtain

$$P_{\rm ph} = c, \tag{56}$$

at both pinholes of the Young interferometer, while across the output plane it turns out to be

$$P_{\rm out}(\xi) = c\frac{1 + \mu_{xy}\cos(2K\xi)}{1 + \mu_{xx}\cos(2K\xi)}. \tag{57}$$

It is worth showing that the latter result can be directly obtained by simply considering the vector modal structure of the field emerging from the Young holes, without resorting to the explicit form of the polarization matrix. In the present case, in fact, the modes $\mathbf{\Psi}_1$ and $\mathbf{\Psi}_3$ are linearly polarized along the same direction (and the same is true for $\mathbf{\Psi}_2$ and $\mathbf{\Psi}_4$) so that the interference pattern consists of a field polarized at $+\pi/4$ with intensity profile given by $I_+ = \lambda_1\cos^2(K\xi) + \lambda_3\sin^2(K\xi)$ and a field polarized at $-\pi/4$ with intensity $I_- = \lambda_2\cos^2(K\xi) + \lambda_4\sin^2(K\xi)$. The resulting degree of polarization is therefore evaluated as

$$\begin{aligned} P_{\rm out}(\xi) &= \frac{I_+ - I_-}{I_+ + I_-} \\ &= \frac{(\lambda_1 - \lambda_2)\cos^2(K\xi) + (\lambda_3 - \lambda_4)\sin^2(K\xi)}{(\lambda_1 + \lambda_2)\cos^2(K\xi) + (\lambda_3 + \lambda_4)\sin^2(K\xi)}, \end{aligned} \tag{58}$$

which, from equation (52), corresponds to the quantity in equation (57). Therefore, even the degree of polarization is an oscillating function of ξ but, differently from the Stokes parameters, it is not sinusoidally modulated. Since $\mu_{xx} \leqslant \mu_{xy}$ (from equations (47) and (45)), its maximum value is reached at the central point of the diffraction pattern, where it equals

$$P_{\rm out}(0) = c\frac{1 + \mu_{xy}}{1 + \mu_{xx}}, \tag{59}$$

which generally differs from $P_{\rm ph}$, unless $\mu_{xy} = \mu_{xx}$, while the minimum, reached half a fringe period away from the centre (at the coordinate, say, $\xi = \xi_{\rm min}$), is

$$P_{\rm out}(\xi_{\rm min}) = c\frac{1 - \mu_{xy}}{1 - \mu_{xx}}. \tag{60}$$

Finally, a *visibility* can be defined even for the degree of polarization and turns out to be

$$V_{\rm pd} = \frac{P(0) - P(\xi_{\rm min})}{P(0) + P(\xi_{\rm min})} = \frac{\mu_{xy} - \mu_{xx}}{1 - \mu_{xx}\mu_{xy}}. \tag{61}$$

4.3. No correlation between orthogonal components

As a last example, we briefly consider the case $c = 0$, which means that there is no correlation between the x and y components of the field impinging onto the Young mask. Furthermore, we put again $a = b = 1$, so that the considered field reproduces the one recently used to study experimentally the relationship between coherence of the field at the pinholes and the polarization degree in the observation plane [19].

Without any loss of generality, we choose as x the axis along which the correlation length between corresponding field

components is maximum, i.e. $\mu_{xx} > \mu_{yy}$. In such a case, it can be easily verified that from equation (33) we have

$$Q_{\pm} = 2 \pm (\mu_{xx} + \mu_{yy}); \qquad R_{\pm} = \mu_{xx} - \mu_{yy}, \tag{62}$$

so that the eigenvalues are

$$\begin{aligned} \lambda_1 &= 1 + \mu_{xx}; & \lambda_2 &= 1 + \mu_{yy}; \\ \lambda_3 &= 1 - \mu_{yy}; & \lambda_4 &= 1 - \mu_{xx}, \end{aligned} \tag{63}$$

while, since in the limit $c \to 0$ both the function ϕ_+ and ϕ_- diverge, the corresponding modes reduce to

$$\begin{aligned} \boldsymbol{\Psi}_1 &= \frac{1}{\sqrt{2}} \begin{bmatrix} 1 \\ 0 \\ 1 \\ 0 \end{bmatrix}, & \boldsymbol{\Psi}_2 &= \frac{1}{\sqrt{2}} \begin{bmatrix} 0 \\ 1 \\ 0 \\ 1 \end{bmatrix}, \\ \boldsymbol{\Psi}_3 &= \frac{1}{\sqrt{2}} \begin{bmatrix} 1 \\ 0 \\ -1 \\ 0 \end{bmatrix}, & \boldsymbol{\Psi}_4 &= \frac{1}{\sqrt{2}} \begin{bmatrix} 0 \\ -1 \\ 0 \\ 1 \end{bmatrix}. \end{aligned} \tag{64}$$

This means that the modes $\boldsymbol{\Psi}_1$ and $\boldsymbol{\Psi}_3$ are polarized along x while $\boldsymbol{\Psi}_2$ and $\boldsymbol{\Psi}_4$ are polarized along y.

Even in this case, the whole polarization matrix, as well as the Stokes parameters, across the observation plane, could be obtained from the modal structure. However, we limit ourselves to the evaluation of the polarization degree. The present situation resembles very closely the one of section 4.2. The modes $\boldsymbol{\Psi}_1$ and $\boldsymbol{\Psi}_3$ as well as $\boldsymbol{\Psi}_2$ and $\boldsymbol{\Psi}_4$ are linearly polarized along the same direction, which now coincides with the x and y axis, respectively. The interference pattern then consists of a field polarized along x with intensity profile given by $I_x = \lambda_1 \cos^2(K\xi) + \lambda_3 \sin^2(K\xi)$ and a field polarized along y with intensity $I_y = \lambda_2 \cos^2(K\xi) + \lambda_4 \sin^2(K\xi)$. The resulting degree of polarization is therefore evaluated as

$$\begin{aligned} P_{\text{out}}(\xi) &= \frac{I_x - I_y}{I_x + I_y} \\ &= \frac{(\lambda_1 - \lambda_2)\cos^2(K\xi) + (\lambda_3 - \lambda_4)\sin^2(K\xi)}{(\lambda_1 + \lambda_2)\cos^2(K\xi) + (\lambda_3 + \lambda_4)\sin^2(K\xi)} \\ &= \frac{\mu_{xx} - \mu_{yy}}{2 + (\mu_{xx} + \mu_{yy})\cos(2K\xi)}, \end{aligned} \tag{65}$$

which is an oscillating function of ξ, so that it does not coincide, in general, with the one at the pinholes (that is, $P_{\text{ph}} = 0$), unless $\mu_{xx} = \mu_{yy}$.

5. Conclusions

The Young interferometer represents the paradigmatical tool for investigating the correlations between the values of a light field at two distinct points, in both the scalar and the electromagnetic analyses. In both cases, in fact, the spatial characteristics of the interference pattern are influenced by the correlation properties of the incident radiation and, conversely, all second-order correlation functions of the incident field can be deduced from measurements on the intensity distribution across the output plane of a suitably modified Young interferometer [2, 13, 37].

The modal theory of coherence for vector fields, applied to two-point sources, offers a useful and easy tool for the study of the relationships between the coherence–polarization properties of the radiation across the output plane of a Young interferometer and those of the beam at the pinholes. We have applied such concepts to the case of a symmetric two-point source, that is a source for which the two points cannot be distinguished from one another on the basis of coherence–polarization measurements involving all the field components at both the points. As an example of such sources we considered a Young interferometer fed by an incident beam of the EGSM type.

In particular, we exploited one of the most useful and intriguing results of the modal theory of coherence, i.e. that any partially coherent and partially polarized field emerging from the Young mask, as well as the one present across the output plane of the interferometer, can always be thought of as originated by the superposition of (at most) four perfectly polarized and mutually uncorrelated modes, having powers proportional to the eigenvalues of the two-point source. This leads, in particular, to the direct evaluation of some parameters of the interference pattern, such as the fringe visibility and the polarization degree. On the other hand, such a model suggests a way to synthesize pairs of electromagnetic fields endowed with prescribed correlation properties starting from the superposition of four mutually uncorrelated perfectly polarized beams.

References

[1] Wolf E 1982 *J. Opt. Soc. Am.* **72** 343–51
[2] Mandel L and Wolf E 1995 *Optical Coherence and Quantum Optics* (Cambridge: Cambridge University Press)
[3] Gori F 1980 *Opt. Commun.* **34** 301–5
[4] Starikov E and Wolf E 1982 *J. Opt. Soc. Am.* A **72** 923–8
[5] Gori F, Guattari G and Padovani C 1987 *Opt. Commun.* **64** 311–6
[6] Gori F, Guattari G, Palma C and Padovani C 1988 *Opt. Commun.* **66** 255259
[7] Simon R, Sundar K and Mukunda M 1993 *J. Opt. Soc. Am.* A **10** 2008–16
[8] Borghi R and Santarsiero M 1998 *Opt. Lett.* **23** 313–5
[9] Borghi R and Santarsiero M 1999 *IEEE J. Quantum Electron.* **35** 745–50
[10] Born M and Wolf E 1999 *Principles of Optics* 7th edn (Cambridge: Cambridge University Press)
[11] James D F V 1994 *J. Opt. Soc. Am.* A **11** 1641–3
[12] Gori F 1998 *Opt. Lett.* **23** 41–3
[13] Gori F, Santarsiero M, Vicalvi S, Borghi R and Guattari G 1998 *Pure Appl. Opt.* **7** 941–51
[14] Wolf E 2003 *Phys. Lett.* A **312** 263–7
[15] Gori F, Santarsiero M, Simon R, Piquero G, Borghi R and Guattari G 2003 *J. Opt. Soc. Am.* A **20** 78–84
[16] Tervo J, Setälä T and Friberg A T 2004 *J. Opt. Soc. Am.* A **21** 2205–15
[17] Roychowdhury H and Wolf E 2005 *Opt. Commun.* **252** 268–74
[18] Réfrégier P and Goudail F 2005 *Opt. Express* **13** 6051–60
[19] Gori F, Santarsiero M, Borghi R and Wolf E 2006 *Opt. Lett.* **31** 688–90
[20] Li Y, Lee H and Wolf E 2006 *Opt. Commun.* **265** 63–72
[21] Setälä T, Tervo J and Friberg A T 2006 *Opt. Lett.* **31** 2208–10
[22] Setälä T, Tervo J and Friberg A T 2006 *Opt. Lett.* **31** 2669–71
[23] Luis A 2006 *J. Opt. Soc. Am.* A **23** 2855–60
[24] Gori F, Santarsiero M and Borghi R 2006 *Opt. Lett.* **31** 858–60
[25] Seshadri S R 1999 *J. Opt. Soc. Am.* A **16** 1373–80
[26] Gori F, Santarsiero M, Piquero G, Borghi R, Mondello A and Simon R 2001 *J. Opt. A: Pure Appl. Opt.* **3** 1–9

[27] Piquero G, Gori F, Romanini P, Santarsiero M, Borghi R and Mondello A 2002 *Opt. Commun.* **208** 9–16
[28] Martínez-Herrero R, Piquero G and Mejías P 2004 *J. Opt. A: Pure Appl. Opt.* **6** S67–71
[29] Shirai T 2005 *Opt. Commun.* **256** 197–209
[30] Korotkova O, Salem M, Dogariu A and Wolf E 2005 *Waves Random Complex Media* **15** 353–64
[31] Roychowdhury H and Korotkova O 2005 *Opt. Commun.* **249** 379–85
[32] Roychowdhury H, Agrawal G and Wolf E 2006 *J. Opt. Soc. Am.* A **23** 940–8
[33] Kim K and Wolf E 2006 *Opt. Commun.* **261** 19–22
[34] Tervo J, Setälä T and Friberg A T 2003 *Opt. Express* **11** 1137–43
[35] Luis A 2007 *J. Opt. Soc. Am.* A **24** 1063–8
[36] Gori F, Santarsiero M and Borghi R 2007 *Opt. Lett.* **32** 588–90
[37] Roychowdhury H and Wolf E 2005 *Opt. Commun.* **226** 57–60